

Manipulating anyons in quantum Hall droplets of light using dissipations

Yangqian Yan, Qi Zhou

Department of Physics and Astronomy, Purdue University, West Lafayette, IN, 47907

(Dated: July 1, 2021)

Whereas anyons are the building blocks in topological quantum computation, it remains challenging to create and control each anyon individually. Here, we point out that dissipative dynamics in cavities deterministically deliver droplets of light in desired fractional quantum Hall states. In these quantum Hall droplets, both the number and locations of anyons are precisely controllable without requiring extra potentials to imprint and localize such quasiparticles. Using the density profile of light, the anyonic statistics is readily accessible. Moreover, entangling a quantum spin valve with these quantum Hall droplets establishes a direct readout of the braiding statistics. Our work unfolds a promising route for quantum optics to solve challenging problems in quantum Hall physics.

It has been a long-lasting goal of physicists to detect anyonic statistics, i.e., exchanging two quasi-particles leads to a phase that is neither 0 nor π [1–4]. Recent experiments have reported direct observations of anyonic statistics in two-dimensional electron gases using either Fabry-Perot interferometers or collisions between anyons at a beamsplitter [5, 6]. In spite of these exciting developments, to fully utilize anyons in quantum computation, it is required to have the capability to manipulate a single anyon in experiments. Such a task remains challenging in two-dimensional electron gases since it is difficult to precisely control the number of anyons in the sample. For instance, neither the number of anyons confined by the gates nor that in the edge currents is unambiguous in typical solid materials. It is thus desired to explore other platforms, in which anyons can be deterministically created and controlled.

Recent progress in quantum optics has provided physicists with an unprecedented opportunity to explore quantum Hall physics using highly controllable photon-atom interactions [7–9]. Synthetic Landau levels have been realized in twisted cavities to access quantum Hall physics in both a flat plane or a cone [8, 10–12]. In the latter case, only a fraction of the lowest Landau levels is occupied, for instance, z_j^{3m} , where $z_j = (x_j + iy_j)$ is the complex coordinate of the j th particle and m is an integer. Strong interactions between photons have been introduced by hybridizing photons with atoms [13–19]. Furthermore, two photons uploaded to a twisted cavity have been prompted to the quantum Hall regime [9]. In parallel, it has been found that the internal state of a single atom in a cavity has been entangled with photons, enabling a new means of quantum spin-valve to control hybridized photon-atom systems [20]. Based on these currently available techniques, here, we point out a scheme to deterministically deliver desired quantum Hall droplets of light, in which both the number and locations of anyons are controllable.

We considered a system identical to that in the Chicago experiment, where N atoms are uploaded to a twisted cavity. In this experiment, these photons are prepared at an initial state $\sim a_m^{\dagger N}|0\rangle$, where a_m^{\dagger} is the creation

operator of a photon at the lowest Landau level (LLL) with an angular momentum m . Whereas a dissipative dynamics turns this trivial initial state into a one in the quantum Hall regime, only one anyon has been created and the position of the anyon is fixed at the origin. This scheme applies to both a cone and a flat plane as shown in Fig. 1(a-b). To levitate constraints to the number and location of anyons in this scheme, we consider an initial state $\sim (\sum_m c_m a_m^{\dagger})^N|0\rangle$, i.e., each photon is prepared at a superposition of multiple angular momenta. This can be easily realized using a pumping laser with multiple angular momentum modes [21]. Such a simple generalization leads to conceptual differences in the resultant quantum Hall droplets. For instance, two anyons could emerge in the droplet, one placed at the origin of a flat plane [Fig. 1(c-d)] or the apex of a cone [Fig. 1(e-f)] and the other separated by a certain distance. A unique advantage of this scheme is that external potentials are not required to localize anyons. In fact, the position of the second anyon is automatically determined by $\{c_m\}$, i.e., the initial condition of the dissipative dynamics. As such, by changing $\{c_m\}$, the position of the second anyon is highly tunable.

We define $|vac\rangle$ as the state with all atoms occupying the s orbital and no photon in the cavity. The time evolution of the density matrix, ρ , of this open system is determined by a master equation [22, 23], $\dot{\rho} = \frac{i}{\hbar}[\rho, H_0 + H_{pump} + U] + \mathcal{D}[\rho]$, where

$$H_0 = \sum_m (gp_m^{\dagger} a_m + \Omega r_m^{\dagger} p_m + h.c.), \quad (1)$$

$$H_{pump} = \sum_m \Omega_m^{pump} (a_m^{\dagger} + a_m). \quad (2)$$

$$\mathcal{D}[\rho] = \sum_m \gamma \left(p_m \rho p_m^{\dagger} - \frac{1}{2} \{ \rho, p_m^{\dagger} p_m \} \right) \quad (3)$$

Replacing m by $3m$, the master equation applies to a cone. The first term in Eq. (1) describes a resonant coupling of the cavity mode with the atoms. To simplify notations, we have used p_m^{\dagger} (r_m^{\dagger}) and p_m (r_m) to denote the atomic transitions between the s orbital and the short-lived p orbital (long-lived Rydberg orbital).

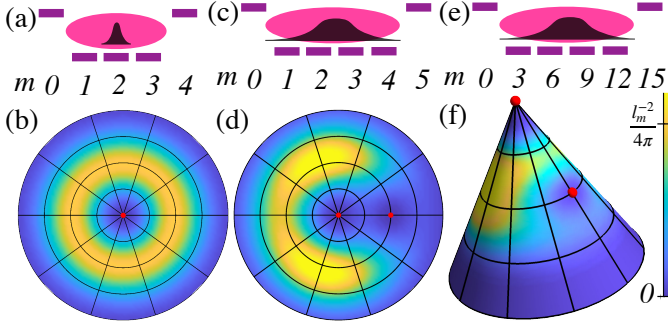


FIG. 1. (a-b) An initial state of photons occupying a single LLL dissipates to a quantum Hall droplet with an anyon fixed at the origin. An appropriate linear combination of multiple LLLs allows the initial state to dissipate to a quantum Hall droplet with two anyons in a flat plane (c-d) and a cone (e-f). The red dots mark the locations of anyons. Density distributions of the droplets are highlighted by colors. The allowed LLLs are constraint between m_{min} and m_{max} .

We have also considered a constant coupling, g . Our results can be directly generalized to m -dependent couplings. The second term in Eq. (1) is induced by an external laser that couples the p state to the Rydberg state with a coupling strength Ω . The subscript of the operators, m , denotes collective excitations of atoms. For instance, $a_m^\dagger = \int_z dz \varphi_m(z) a_z^\dagger$, where $z = (x + iy)/\ell_m$ is the real space coordinate, $\varphi_m(z) = \frac{1}{\sqrt{\pi m! \ell_m}} z^m e^{-|z|^2/2}$ is the wavefunction with an angular momentum m in the LLL, and a_z^\dagger is the operator for photons at position z . The magnetic length ℓ_m has been set to 1. p_m^\dagger and r_m^\dagger can be expressed in terms of operators in the real space in a similar manner.

Because of the diluteness of the atoms inside the cavity, the interaction between two Rydberg atoms is well modeled by a contact interaction U [24] and the interactions between two atoms at the s and p orbitals are negligible,

$$U = U_0 \sum_{\{m_i\}} U_{m_1, m_2}^{m_3, m_4} r_{m_1}^\dagger r_{m_2}^\dagger r_{m_3} r_{m_4}, \quad (4)$$

$$U_{m_1, m_2}^{m_3, m_4} = \frac{(m_1 + m_2)!}{2\pi 2^{m_1 + m_2} \sqrt{m_1! m_2! m_3! m_4!}}. \quad (5)$$

In Eq. (3), γ describes the decay of atoms in the short-lived p orbital, and Ω_{pump} denotes the strength of an additional field that continuously pump photons to the cavity. Again, γ has been treated as a constant for simplicity. We first consider a vanishing pump, $\Omega_m = 0$. The initial state, $|\Psi_I\rangle = (\sum_m c_m a_m^\dagger)^N |vac\rangle / \sqrt{N!}$, can be rewritten in the coordinate space as

$$|\Psi_I\rangle = \mathcal{N}_I^{-\frac{1}{2}} \int \prod_i dz_i \Psi_I(\{z_i\}) a_{z_i}^\dagger |vac\rangle, \quad (6)$$

where $\Psi_I(\{z_i\}) = \prod_{i=1}^N (\sum_m c_m \varphi_m(z_i))$, $\{z_i\}$ is a shorthand notation for $\{z_1, z_2, \dots, z_N\}$, and \mathcal{N}_I is the normalization factor. For $N = 1$, it is easy to see that all bright states vanish at long times, and the initial state decays to a one-body zero-energy dark polariton state,

$$\rho_I = |\Psi_I\rangle \langle \Psi_I| \xrightarrow{t \gg \gamma^{-1}} \rho_F^o = |\Psi_F^o\rangle \langle \Psi_F^o|, \quad (7)$$

$$|\Psi_F^o\rangle = \lambda \int dz \left(\sum_m c_m \varphi_m \right) d_z^\dagger |vac\rangle, \quad (8)$$

where $\lambda = \frac{\Omega}{\sqrt{\Omega^2 + g^2}}$ and $d_z^\dagger = \lambda a_z^\dagger - \frac{g\lambda}{\Omega} r_z^\dagger$ is the creation operator for a dark state at z (Supplemental Materials). Since the p orbital is not involved, $|\Psi_F^o\rangle$ as a superposition of eigenstates of H_0 survives the dissipative dynamics.

When $N > 1$, a N -polariton zero-energy dark states, $|D_l\rangle$, is labeled by l , the angular momentum that is conserved in the dissipative dynamics. $|D_l\rangle$ satisfies two criteria. First, it must be constructed by only one-body dark polariton states. Otherwise, the p orbital will be present and causes decay. Second, its spatial wavefunction must vanish when two dark polaritons sit on top of each other. Otherwise, the finite interaction energy leads to an off-resonant condition such that this state cannot be excited. As such, in the long time limit, the dissipative dynamics in the cavity amounts to projecting the initial state to a superposition of $|D_l\rangle$ with zero-energies,

$$|\Psi_F\rangle = \sum_l \tilde{u}_l |D_l\rangle, \quad (9)$$

$$|D_l\rangle = \int \prod_{i=1}^N dz_i \phi_l(\{z_i\}) \prod_i d_{z_i}^\dagger |vac\rangle, \quad (10)$$

where $\tilde{u}_l = \langle D_l | \Psi_I \rangle$ [25], and $\phi_l(\{z_i\}) = 0$ when $z_j = z_k$ for any $j \neq k$ (Supplemental Materials). The above discussions show that, if an appropriate $|\Psi_F\rangle$ is chosen, the corresponding u_l could deliver a target state of interest.

As an example, we show how to obtain a N -polariton state in a flat plane with two anyons, i.e., two quasi-holes,

$$|\Phi\rangle = \int \prod_i dz_i \Phi(\{z_i\}) \prod_i d_{z_i}^\dagger |vac\rangle, \quad (11)$$

$$\Phi(\{z_i\}) = \mathcal{N}^{-\frac{1}{2}} \prod_{i=1}^N z_i (z_i - \eta) \prod_{i < j} (z_i - z_j)^2 \prod_i e^{-\frac{|z_i|^2}{2}},$$

where

the first anyon is located at $z = 0$ and the other at $z = \eta$. All results can be immediately generalized to a cone by replacing z_i by z_i^3 .

Expanding $\Phi(\{z_i\})$ in terms of η , we see that it is a superposition of multiple zero-energy states,

$$\Phi(\{z_i\}) = \mathcal{N}^{-\frac{1}{2}} \left(\sum_{l=N^2}^{N^2+N} (-\eta)^{N^2+N-l} \phi_l \right), \quad (12)$$

where

$$\phi_{N^2}(\{z_i\}) = \prod_{i=1}^N z_i \prod_{i<j} (z_i - z_j)^2 \prod_i e^{-|z_i|^2/2}, \quad (13)$$

$$\phi_l(\{z_i\}) = \left(\sum_{i_1, i_2, \dots, i_{N-(N^2-l)}} \prod_{k=1}^{N-(N^2-l)} z_{i_k} \right) \phi_{N^2}(\{z_i\}). \quad (14)$$

Apparently, each $\phi_l(\{z_i\})$ vanishes whenever two particles have identical coordinates and thus have a zero interaction energy. It carries a unique total angular momentum l , and Φ is a superposition of multiple states with different angular momenta, $l = N^2, N^2 + 1, \dots, N^2 + N$, when $\eta \neq 0$. Interestingly, each $\phi_l(\{z_i\})$ is precisely a Jack polynomial, a powerful tool that has been extensively studied in quantum Hall physics (Supplemental Materials).

To access $|\Phi\rangle$ at long times in the dissipative dynamics, we required that the allowed single-particle states in the LLL are $m = 1, 2, \dots, N$. As such, the initial state is written as

$$\Psi_{\text{I}}(\{z_i\}) = \mathcal{N}_{\text{I}}^{-\frac{1}{2}} \prod_{i=1}^N \left(z_i^{(N+1)} + \sum_{m=1}^N c_m z_i^m \right) \prod_i e^{-|z_i|^2/2}, \quad (15)$$

which depends on N parameters. Apparently, Ψ_{I} is also a superposition of multiple states with angular momenta $N, \dots, N^2 + N$,

$$\Psi_{\text{I}} = \sum_{l=N}^{N^2+N} \psi_l(\{z_i\}). \quad (16)$$

When $l < N^2$, there does not exist a state in LLL with vanishing contact interaction energy as long as single-particle $m = 0$ states are excluded. Thus, any $\psi_{l < N^2}(\{z_i\})$ can only be turned into bright states and eventually be dissipated away. When $N^2 \leq l \leq N^2 + N$, $\phi_l(\{z_i\})$ is only zero energy eigenstate for each l , provided that the available single-particle states are constrained between $m_{\text{min}} = 1$ and $m_{\text{max}} = N + 1$. The cutoffs, $m_{\text{min}} = 1$ and $m_{\text{max}} = N + 1$, can be provided by either the finite size of the mirror or purposely limiting available angular momentum channels [23], as shown in Fig. 1. Therefore, $\psi_l(\{z_i\})$, which has a fixed angular momentum l , must decay to $\phi_l(\{z_i\})$ in long times.

We denote the overlap between $\psi_l(\{z_i\})$ and ϕ_l as μ_l ,

$$u_l = \frac{\int \prod_i dz_i \phi_l^*(\{z_i\}) \psi_l(\{z_i\})}{\int \prod_i dz_i \phi_l^*(\{z_i\}) \phi_l(\{z_i\})} \quad (17)$$

To ensure that $\Psi_{\text{I}}(\{z_i\})$ in Eq. (16) eventually dissipates to $\Phi(\{z_i\})$ as shown in Eq. (12), it is required that

$$u_l(c_1, c_2, \dots, c_N) = -\eta u_{l+1}(c_1, c_2, \dots, c_N), \quad (18)$$

$$l = N^2, \dots, N^2 + N - 1. \quad (19)$$

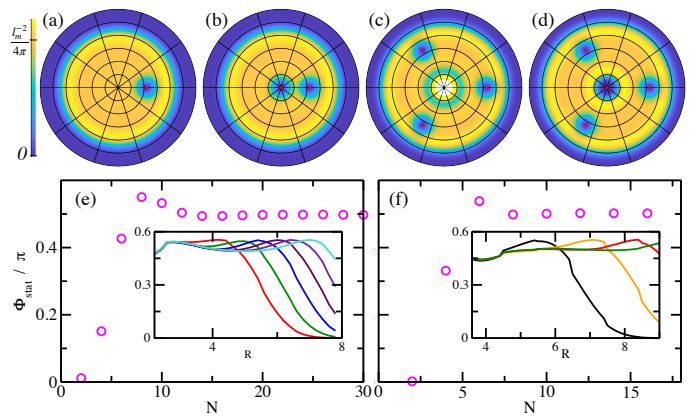


FIG. 2. Radial density $\rho(r)$ for one-quasihole (ac) state and two-quasihole (bd) state. Panel (ab) are for the flat space and (cd) are for a cone with $\delta m = 3$. The radial spacing is $2l_m$. The density is normalized to the number of particles $N = 20$ ($N = 8$) for panel (ab) [(cd)]. Panel (e) [(f)] show the statistical phase factor as a function of N in a flat space (cone) while fixing $r = 4.4$ ($r = 6.6$). Insets show the statistical phase factor as a function of r . Black, orange, red, green, blue, brown, purple, cyan lines are for $N = 4, 6, 8, 10, 12, 14, 16, 18$. The red dots mark the locations of anyons. Due to the curvature singularity at the cone tip, the density at the origin of panel (c) reaches $5.6l_m^{-2}/(4\pi)$, which exceeds the color scale. Thus, this region is excluded from the density plot.

Since there are in together N such equations, we could then uniquely determine the N unknown parameters in Eq. (15). For instance, if $N = 2$, we find that $c_1 = -4\eta^2/25$, $c_2 = -9\eta/10$. A few other examples of the explicit expressions of c_m are given in the supplemental materials. In fact, $\psi_l(\{z_i\})$ in the initial state can also be written in terms of Jack polynomials so as to simplify numerics (Supplemental Materials). When Eq. (19) is satisfied, we conclude that

$$|\Psi_{\text{I}}\rangle \xrightarrow{t \gg \gamma^{-1}} \lambda^N \mathcal{N}_{\text{I}}^{-\frac{1}{2}} \mathcal{N}^{\frac{1}{2}} |\Phi\rangle, \quad (20)$$

i.e., the dissipative dynamics turns initial state into desired quantum Hall states. Here the λ^N factor originates from the overlap between the single-particle photonic state and the dark-polariton state.

The same scheme could be applied to a quasi-hole state of N polaritons on a cone by tuning δm , or the creation of a single quasi-hole state at location η (Supplemental Materials).

The dissipative dynamics at long times as discussed above can be verified by numerically solving the master equation, from which the density matrix at any given time is obtained. Since the numerics is heavy for $N > 2$, we focus on $N = 2$ when solving the master equation. We do observe that starting from a 2-body state, $(a_1^\dagger)^2 |vac\rangle$, the final 2-body state that survives the dissipative dynamics is indeed the quasihole state at the origin (Supplemental Materials). Nevertheless, we would like to point

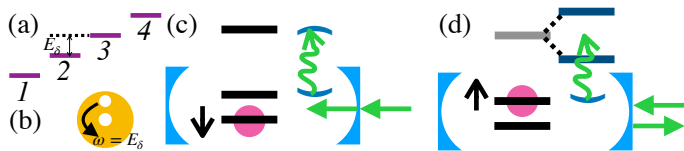


FIG. 3. (a) Tilting the single-particle angular momentum levels results in the rotation of hole (b). (c-d) illustrates the coupling of a quantum spin valve with a many-body state. (c) While the spin is down, light can enter the cavity. (d) While the spin is up, light is reflected off due to off-resonance condition. As the number of particles increases, the statistical phase factor approaches 0.5π . Inset shows the statistical phase factor as a function of R for $N = 20$.

out that the full solution of the master equation includes a mixture of density matrices with different total particle numbers. In addition to the N -body sector, other sectors with particle numbers ranging from 0 to N also exist. The same analysis can be performed for each sector, which hosts certain quantum Hall states with less than N particles. Alternatively, a simpler solution is to turn on Ω^{pump} . The steady state is a superposition of states with the number of photons centered around N [26]. Choosing the appropriate single momentum cutoffs, the $N + i$ photon sector with $i > 0$ does not have zero energy state, under strong interaction and large p -wave decay, they will decay thus N -photon event must come from the N -body sector.

We now turn to the measurement of anyonic statistics. The simplest way is to measure the density profile of the quasi-hole state. It is known that moving a single hole around a loop, the many-body wavefunction accumulates a phase proportional to the total particle number enclosed by the loop with a radius R [27]. Adding an extra hole inside this loop, half of the change of such geometric phase precisely provides us with the statistic phase of the anyons,

$$\phi_{\text{stat}} = \int_0^R \pi(\rho_{1,\eta}(r) - \rho_{2,\eta}(r))dr, \quad (21)$$

where $\rho_{1,\eta}$ is the density of the state with one hole located at $z = \eta$ and $\rho_{2,\eta}$ is that of the state with an additional hole at the origin [28]. Thus, comparing the density profiles of these two quantum Hall states readily allows us to extract the abelian statistic phase. In practice, however, a key question is the finite size effect as Eq. (21) is obtained in the thermodynamic limit where the size of the hole is negligible. As shown in Fig. 2, on both the flat space and the cone, when $N = 20$, the density at the plateau is readily close to $1/2$, indicating that such particle number is readily a good approximation for the results in the thermodynamic limit. The inset of Fig. 3(c) shows the statistical phase factor over π as a function of cutoff radius R . A plateau where anyonic statistics is robust is already clear. A more rigorous means is to trace

the dependence of the height of the plateau as a function of N , from which the result at $N \rightarrow \infty$ can be extrapolated [Fig. 3(c)]. Considering the cone leads to smaller required N [29] [Fig 3(d)]. For example, ϕ_{stat} on a cone shows a plateau at $N = 8$ and 10 . For $N = 4$ and $N = 6$, we can already find a regime of r where ϕ_{stat} is close to 0.5 .

A more direct means of measuring the anyonic statistics is to braid two anyons, i.e., moving one around the other. The anyonic statistics encoded by the overlap between two many-body wavefunctions, one with anyons braided and the other without such a braiding, is then transferred to a quantum spin-valve. Similar ideas of using a single spin to measure quantum coherence in many-body systems have been studied for various purposes [20, 30–33]. Here, measuring the spin coherence of the quantum spin-valve, the anyonic statistics can be extracted. Whereas this scheme is very generic, here, we consider a quantum spin-valve in a cavity to concretize the discussions [20]. To this end, we consider the quasi-hole state leaked out from the cavity where it is created. Then only the photonic part of the state is relevant and the spatial part of the wavefunction remains unchanged. Such quasi-hole state of photons is transferred to another cavity, which includes a quantum spin-valve. This quantum spin-valve is made of a single atom, whose hyperfine spin state controls whether the quantum Hall state of photons could enter the cavity. When it is spin-up (down), photons can (cannot) enter the cavity, similar to the experiment in reference [20]. Thus, when the quantum spin-valve is prepared at a superposition of up and down, two copies of the quasi-hole state of photons is created, $|\Phi\rangle = \frac{1}{\sqrt{2}}(|\uparrow\rangle|\Phi_\eta\rangle + |\downarrow\rangle|\Phi_\eta\rangle)$, where the copy combined with spin-up(down) is inside (outside) the cavity.

Inside the cavity, we now tilt LLL such that it is no longer flat and the single particle energy becomes $\sum_m mE_\delta a_m^\dagger a_m$, where E_δ is a constant energy. After tilting LLL for a certain time t , each ϕ_l in Eq. (S5) acquires a dynamical phase, $e^{-iE_\delta l t}$. This phase can then be absorbed by η such that $\eta \rightarrow \eta' = \eta e^{-i\omega t}$. Thus, as time goes by, one hole encircle the other with an angular frequency, $\omega = E_\delta$, without requiring an external force to drag it, as shown in Fig. 1(d). Meanwhile, the copy outside the cavity remains unchanged. After a certain time t , the wavefunction becomes $|\Phi'\rangle = \frac{1}{\sqrt{2}}(|\uparrow\rangle|\Phi_{\eta'}\rangle + |\downarrow\rangle|\Phi_\eta\rangle)$. At this time, the coherence of the quantum spin-valve is given by $\langle\downarrow|\uparrow\rangle = \frac{1}{2}\mathcal{F} \equiv \frac{1}{2}\langle\Phi_\eta|\Phi_{\eta'}\rangle$. In other words, the overlap between two quasi-hole states, \mathcal{F} , is encoded in the quantum spin-valve. In particular, when η and η' are close to each other, i.e., t is small, the Berry connection can be obtained from \mathcal{F} . In this particular braiding scheme, only the amplitude of η changes, and $\vec{A} = A\hat{\theta}$, where $\theta = \arg \eta$, $\hat{\theta}$ is the unit vector in the angular direction, and $A = i\langle\Phi_\eta|\nabla_\theta|\Phi_\eta\rangle/|\eta|$. It is straightforward

to see that $A = i(1 - \mathcal{F})/(\arg \eta - \arg \eta')$. Once \vec{A} is obtained for each θ , a loop integral of \vec{A} then delivers the total geometric phase accumulated by braiding the anyons.

To summarize, we propose to use dissipation to transform a trivial product state with mixed angular momentums to an entangled few-body Laughlin states with quasihole excitations. Tuning the initial mixing of the angular momentum states, up to two quasipoles could be generated. The anyonic statistics could then be verified indirectly by measuring the density distribution or directly by braiding. We hope the few-body version of the non-abelian anyonic state could be engineered in the future.

This work is supported by the Air Force Office of Scientific Research under award number FA9550-20-1-0221 and a seed grant from PQSEI.

-
- [1] B. Paredes, P. Fedichev, J. I. Cirac, and P. Zoller, 1/2-anyons in small atomic bose-einstein condensates, *Phys. Rev. Lett.* **87**, 010402 (2001).
- [2] A. Y. Kitaev, Fault-tolerant quantum computation by anyons, *Ann. Phys.* **303**, 2 (2003).
- [3] C. Nayak, S. H. Simon, A. Stern, M. Freedman, and S. Das Sarma, Non-abelian anyons and topological quantum computation, *Rev. Mod. Phys.* **80**, 1083 (2008).
- [4] S. Dutta and E. J. Mueller, Coherent generation of photonic fractional quantum hall states in a cavity and the search for anyonic quasiparticles, *Phys. Rev. A* **97**, 033825 (2018).
- [5] H. Bartolomei, M. Kumar, R. Bisognin, A. Marguerite, J.-M. Berroir, E. Bocquillon, B. Plaças, A. Cavanna, Q. Dong, U. Gennser, Y. Jin, and G. Fève, Fractional statistics in anyon collisions, *Science* **368**, 173 (2020).
- [6] J. Nakamura, S. Liang, G. C. Gardner, and M. J. Manfra, Direct observation of anyonic braiding statistics, *Nat. Phys.* **16**, 931 (2020).
- [7] N. Jia, N. Schine, A. Georgakopoulos, A. Ryou, A. Sommer, and J. Simon, A strongly interacting polaritonic quantum dot, *Nat. Phys.* **14**, 550 (2018).
- [8] T. Ozawa, H. M. Price, A. Amo, N. Goldman, M. Hafezi, L. Lu, M. C. Rechtsman, D. Schuster, J. Simon, O. Zeitler, and I. Carusotto, Topological photonics, *Rev. Mod. Phys.* **91**, 015006 (2019).
- [9] L. W. Clark, N. Schine, C. Baum, N. Jia, and J. Simon, Observation of laughlin states made of light, *Nature* **582**, 41 (2020).
- [10] L. Lu, J. D. Joannopoulos, and M. Soljačić, Topological photonics, *Nat. Photon.* **8**, 821 (2014).
- [11] N. Schine, A. Ryou, A. Gromov, A. Sommer, and J. Simon, Synthetic landau levels for photons, *Nature (London)* **534**, 671 (2016).
- [12] N. Jia, N. Schine, A. Georgakopoulos, A. Ryou, A. Sommer, and J. Simon, Photons and polaritons in a broken-time-reversal nonplanar resonator, *Phys. Rev. A* **97**, 013802 (2018).
- [13] M. D. Lukin, Colloquium: Trapping and manipulating photon states in atomic ensembles, *Rev. Mod. Phys.* **75**, 457 (2003).
- [14] K. M. Birnbaum, A. Boca, R. Miller, A. D. Boozer, T. E. Northup, and H. J. Kimble, Photon blockade in an optical cavity with one trapped atom, *Nature (London)* **436**, 87 (2005).
- [15] I. Fushman, D. Englund, A. Faraon, N. Stoltz, P. Petroff, and J. Vučković, Controlled phase shifts with a single quantum dot, *Science* **320**, 769 (2008).
- [16] T. Peyronel, O. Firstenberg, Q.-Y. Liang, S. Hofferberth, A. V. Gorshkov, T. Pohl, M. D. Lukin, and V. Vuletić, Quantum nonlinear optics with single photons enabled by strongly interacting atoms, *Nature (London)* **488**, 57 (2012).
- [17] D. E. Chang, V. Vuletić, and M. D. Lukin, Quantum nonlinear optics — photon by photon, *Nat. Photon.* **8**, 685 (2014).
- [18] O. Firstenberg, C. S. Adams, and S. Hofferberth, Nonlinear quantum optics mediated by rydberg interactions, *J. Phys. B* **49**, 152003 (2016).
- [19] M. J. Hartmann, Quantum simulation with interacting photons, *J. Opt.* **18**, 104005 (2016).
- [20] A. Reiserer, S. Ritter, and G. Rempe, Nondestructive detection of an optical photon, *Science* **342**, 1349 (2013).
- [21] For example: N. K. Fontaine, R. Ryf, H. Chen, D. T. Neilson, K. Kim, and J. Carpenter, Laguerre-gaussian mode sorter, *Nat. Commun.* **10**, 1 (2019).
- [22] C. Cohen-Tannoudji, J. Dupont-Roc, and G. Grynberg, *Atom-photon interactions: basic processes and applications* (Wiley, New York, 1992).
- [23] L. W. Clark, N. Jia, N. Schine, C. Baum, A. Georgakopoulos, and J. Simon, Interacting floquet polaritons, *Nature (London)* **571**, 532 (2019).
- [24] M. Popp, B. Paredes, and J. I. Cirac, Adiabatic path to fractional quantum hall states of a few bosonic atoms, *Phys. Rev. A* **70**, 053612 (2004).
- [25] B. Juliá-Díaz and T. Graß, Strongdeco: Expansion of analytical, strongly correlated quantum states into a many-body basis, *Comp. Phys. Comm.* **183**, 737 (2012).
- [26] It is known that the interplay between the pumping field and the dissipation could establish a quasi-equilibrium in a cavity such that the number of photons or polaritons is concentrated around a narrow peak at N with variance \sqrt{N} . M. Fox, *Quantum Optics: An Introduction*, Oxford Master Series in Physics (Oxford University Press, Oxford, New York, 2006).
- [27] D. Arovas, J. R. Schrieffer, and F. Wilczek, Fractional statistics and the quantum hall effect, *Phys. Rev. Lett.* **53**, 722 (1984).
- [28] The density is defined as $\rho_{j,\eta}(r) = \int_0^\infty |\Psi_{j,\eta}|^2 \sum_i \delta(|z_i| - r) \prod_{i=1}^N dz_i$. The normalization gives N , i.e., $\int_0^\infty \rho_{i,\eta} = N$. The geometric phase difference is $\Delta\phi = \int_0^R 2\pi(\rho_{1,\eta}(r) - \rho_{2,\eta}(r))dr$, Circling one hole around another by a loop is equivalent to exchange twice, i.e., $\phi_{\text{stat}} = \Delta\phi/2$.
- [29] Y.-H. Wu, H.-H. Tu, and G. J. Sreejith, Fractional quantum hall states of bosons on cones, *Phys. Rev. A* **96**, 033622 (2017).
- [30] H. T. Quan, Z. Song, X. F. Liu, P. Zanardi, and C. P. Sun, Decay of loschmidt echo enhanced by quantum criticality, *Phys. Rev. Lett.* **96**, 140604 (2006).
- [31] R. Hanson, V. V. Dobrovitski, A. E. Feiguin, O. Gywat, and D. D. Awschalom, Coherent dynamics of a single spin interacting with an adjustable spin bath, *Science*

- 320, 352 (2008).**
- [32] B.-B. Wei and R.-B. Liu, Lee-yang zeros and critical times in decoherence of a probe spin coupled to a bath, *Phys. Rev. Lett.* **109**, 185701 (2012).
 - [33] D. V. Vasilyev, A. Grankin, M. A. Baranov, L. M. Sieberer, and P. Zoller, Monitoring quantum simulators via quantum nondemolition couplings to atomic clock qubits, *PRX Quantum* **1**, 020302 (2020).
 - [34] B. A. Bernevig and F. D. M. Haldane, Model fractional quantum hall states and jack polynomials, *Phys. Rev. Lett.* **100**, 246802 (2008).
 - [35] L. Lapointe, A. Lascoux, and J. Morse, Determinantal expression and recursion for jack polynomials, *Electron. J. Combin.* **7**, N1 (2000).

Supplemental Material of “Manipulating anyons in quantum Hall droplets of light using dissipations”

In this supplemental material, we present results of the one-body dark state, Jack polynomials for both one and two quasi-hole states, mapping initial state to monomial basis, and solutions to the master equation.

THE ONE-BODY DARK STATE

The spatial wave function in first quantization form reads $\Psi_1(\{z_i\}) = \prod_{i=1}^N (\sum_m c_m \varphi_m(z_i))$. Though Eq. (3) from the main text can be solved numerically, it is useful to analytically study what state survive the dissipative dynamics at long times. When $N = 1$, we see from Eq. (1) from the main text that the eigenstate of H_0 can be written as $|D_m\rangle = d_m^\dagger |vac\rangle$, $|B_{m,\pm}\rangle = b_{m,\pm}^\dagger |vac\rangle$, and

$$\begin{aligned} d_m^\dagger &= \lambda a_m^\dagger - \frac{g\lambda}{\Omega} r_m^\dagger, \\ b_{m,\pm}^\dagger &= \frac{g\lambda}{\sqrt{2}\Omega} a_m^\dagger + \frac{\lambda}{\sqrt{2}} r_m^\dagger \pm \frac{1}{\sqrt{2}} p_m^\dagger. \end{aligned} \quad (S1)$$

where $\lambda = \frac{\Omega}{\sqrt{\Omega^2 + g^2}}$. Apparently, the dark state, $|D_m\rangle$, of a polariton is immune to the dissipation as it does not contain the p orbital. The two bright states of polaritons, $|B_{m,\pm}\rangle$, eventually decay and will not contribute to the final density matrix when $t \gg 1/\gamma$. If we use $|\Psi_1^o\rangle$ to denote the initial state of a single particle, all bright states vanish at long times, and

$$|\Psi_1^o\rangle \xrightarrow{t \gg \gamma^{-1}} \lambda \int dz \left(\sum_m c_m \varphi_m(z) \right) d_z^\dagger |vac\rangle, \quad (S2)$$

where $d_m^\dagger = \int dz \varphi_m(z) d_z^\dagger$, and $d_z^\dagger = \sum_m \varphi_m^*(z) d_m^\dagger$.

JACK POLYNOMIALS AND QUANTUM HALL STATES

The wave function of the quasihole state carrying a single quasihole is written as

$$\Phi_{1,\eta}(\{z_i\}) = \mathcal{N}_1^{-\frac{1}{2}} \prod_{i=1}^N (z_i - \eta) \prod_{i < j} (z_i - z_j)^2 \prod_i e^{-\frac{|z_i|^2}{2}}, \quad (S3)$$

where

η denotes the location of quasihole. When η is finite, this state is a superposition of multiple angular momentum states. Expanding Eq. (S3) in power series of η , we obtain

$$\Phi_{1,\eta}(\{z_i\}) = \mathcal{N}_1^{-\frac{1}{2}} \left(\sum_{l=N^2-N}^{N^2} (-\eta)^{N^2-l} \phi_l(\{z_i\}) \right) \prod_i e^{-|z_i|^2/2}, \quad (S4)$$

where

$$\phi_l(\{z_i\}) = \left(\sum_{i_1, i_2, \dots, i_{N-(N^2-l)}} z_{i_1} z_{i_2} \dots z_{i_{N-(N^2-l)}} \right) \phi_{N^2-N}(\{z_i\}).$$

Each state $\phi_l(\{z_i\})$ has a fixed angular momentum, l . For instance, when $N = 3$, $\Phi_{1,\eta}(z_1, z_2, z_3) = \mathcal{N}_1^{-\frac{1}{2}} \left(\sum_{l=6}^9 (-\eta)^{N^2-l} \phi_l(z_1, z_2, z_3) \right) e^{-(|z_1|^2 + |z_2|^2 + |z_3|^2)/2}$, and

$$\begin{aligned} \phi_6 &= (z_1 - z_2)^2 (z_2 - z_3)^2 (z_3 - z_1)^2, \\ \phi_7 &= (z_1 + z_2 + z_3) (z_1 - z_2)^2 (z_2 - z_3)^2 (z_3 - z_1)^2, \\ \phi_8 &= (z_1 z_2 + z_2 z_3 + z_3 z_1) (z_1 - z_2)^2 (z_2 - z_3)^2 (z_3 - z_1)^2, \\ \phi_9 &= z_1 z_2 z_3 (z_1 - z_2)^2 (z_2 - z_3)^2 (z_3 - z_1)^2. \end{aligned} \quad (S5)$$

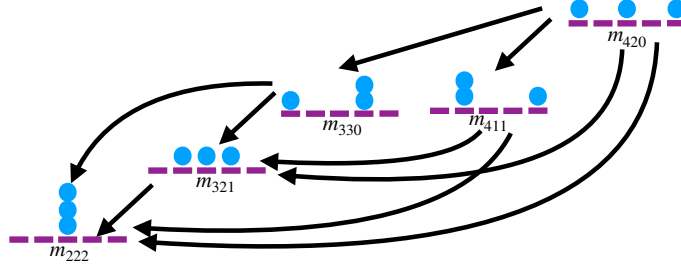


FIG. S1. Repeatedly applying the squeeze operator to the Jack polynomial of m_{420} generates all other polynomials for total angular momentum $l = 6$.

It turns out that $\phi_l(\{z_i\})$ corresponds to a Jack polynomial $J_\lambda^\alpha(\{z_i\})$ [34]. A Jack polynomial [35], which has N arguments, $\{z_i\} \equiv \{z_1, z_2, \dots, z_N\}$, depends on a number of indices. One of them is denoted by α . For relevant states in our case, $\alpha = -2$. For the Moore-Read and other quantum Hall states, α takes different values. λ , a short-hand notation for a set of indices, $\{\lambda_1, \lambda_2, \dots, \lambda_N\}$, where $\lambda_1 \geq \lambda_2 \geq \lambda_3 \geq \dots \geq \lambda_N$, depends on the angular momentum, l , and the total particle number, N . If we denote l as $l = N(N-1) + l_r$ with $l_r > 0$, the explicit expression of λ_i can be written as

$$\lambda_i = \begin{cases} 2N - 2i + 1, & i < l_r, \\ 2N - 2i, & i \geq l_r. \end{cases}$$

$\lambda = \{\lambda_1, \lambda_2, \dots, \lambda_N\}$ specifies one of the monomials in the Jack polynomial,

$$m_\lambda = \frac{1}{\prod_{k=0}^{\infty} (n_k!)} \text{Permanant}(z_i^{\lambda_i}), \quad (\text{S6})$$

where n_k is the number of times for the integer k to appear in $\{\lambda_1, \lambda_2, \dots, \lambda_N\}$. For instance, $m_{420} = (z_1^4 z_2^2 z_3^0 + z_2^4 z_3^2 z_1^0 + z_3^4 z_1^2 z_2^0)$. Each of these three integers, 4, 2, 0, shows up in $\lambda = \{4, 2, 0\}$ once and any other integer does not exist. As such, $\prod_{k=0}^{\infty} (n_k!) = 1$ in this example. All other monomials in a Jack polynomial can be derived from m_λ by squeezings.

The explicit expression of a Jack Polynomial can be written in terms of a determinant,

$$J_\lambda^\alpha = \frac{1}{\mathcal{N}_{J_\lambda^\alpha}} \begin{vmatrix} m_{\lambda^{(1)}} & m_{\lambda^{(2)}} & \cdots & \cdots & m_{\lambda^{(n-1)}} & m_{\lambda^{(n)}} \\ d_{\lambda^{(1)}} - d_{\lambda^{(n)}} & C_{\lambda^{(2)}\lambda^{(1)}} & \cdots & \cdots & C_{\lambda^{(n-1)}\lambda^{(1)}} & C_{\lambda^{(n)}\lambda^{(1)}} \\ 0 & d_{\lambda^{(2)}} - d_{\lambda^{(n)}} & & & \cdots & C_{\lambda^{(n)}\lambda^{(2)}} \\ \vdots & 0 & \ddots & & & \vdots \\ \vdots & \vdots & \ddots & \ddots & & \vdots \\ 0 & 0 & \cdots & 0 & d_{\lambda^{(n-1)}} - d_{\lambda^{(n)}} & C_{\lambda^{(n)}\lambda^{(n-1)}} \end{vmatrix}, \quad (\text{S7})$$

where $\lambda^{(n)} \equiv \lambda$. A squeezing operation, which allows two particles to exchange a certain amount of angular momentum, changes $m_{\lambda^{(n)}}$ to another monomial, such as $m_{\lambda^{(n-1)}}$. For instance, m_{420} becomes m_{411} after applying a squeezing operation in which the angular momentum of one particle decreases from 2 to 1 and correspondingly the angular momentum of the other one increases from 0 to 1, i.e., $\lambda^{(n)} = \{4, 2, 0\}$ has become $\lambda^{(n-1)} = \{4, 1, 1\}$. Repeating the squeezing operations to $\lambda^{(n)}$, or other states obtained from previous squeezings, all states in the first row of the above equation are obtained. Fig. S1 shows an example of how to obtain all states from squeezing m_{420} . These $m_{\lambda^{(i)}}$ are ordered based on $\lambda^{(1)} < \lambda^{(2)} < \dots < \lambda^{(n)}$. $\lambda^{(j)} < \lambda^{(k)}$ means that there exist a i^* such that $\lambda_{i^*}^{(j)} \leq \lambda_{i^*}^{(k)}$ for any $i \leq i^*$. For instance, the states in Fig. S1 are ordered as $m_{222}, m_{321}, m_{330}, m_{411}, m_{420}$.

In Eq.(S7), the upper triangle excluding the first row is defined as

$$C_{\lambda^{(j)}\lambda^{(k)}} = \begin{cases} \left(\lambda_{i_1}^{(j)} - \lambda_{i_2}^{(j)} \right) \binom{n(\lambda_{i_1}^{(k)})}{2} & \text{if } \lambda_{i_1}^{(k)} = \lambda_{i_2}^{(k)} \\ \left(\lambda_{i_1}^{(j)} - \lambda_{i_2}^{(j)} \right) n(\lambda_{i_1}^{(k)}) n(\lambda_{i_2}^{(k)}) & \text{if } \lambda_{i_1}^{(k)} \neq \lambda_{i_2}^{(k)} \end{cases} \quad (\text{S8})$$

where $\lambda_{i_1}^{(k)} = \lambda_{i_1}^{(j)} - k$, $\lambda_{i_2}^{(k)} = \lambda_{i_2}^{(j)} + k$, $0 \leq \lambda_{i_2}^{(j)} < \lambda_{i_1}^{(j)}$ and $0 < k \leq (\lambda_{i_1}^{(j)} - \lambda_{i_2}^{(j)})/2$. As shown in Fig. S1, $\lambda_{i_1}^{(j)}$ and $\lambda_{i_2}^{(j)}$ are the ones in $\lambda^{(j)} = \{\lambda_1^{(j)}, \lambda_2^{(j)}, \dots, \lambda_N^{(j)}\}$ that change to $\lambda_{i_1}^{(k)}$ and $\lambda_{i_2}^{(k)}$ in a squeezing from $\lambda^{(j)}$ to $\lambda^{(k)}$. $n(\lambda_{i_1}^{(k)})$ is the number of times that $\lambda_{i_1}^{(k)}$ shows up in $\lambda^{(k)} = \{\lambda_1^{(k)}, \lambda_2^{(k)}, \dots, \lambda_N^{(k)}\}$.

The final next-to-diagonal line is defined as

$$d_{\lambda^{(j)}} - d_{\lambda^{(k)}} = \sum_{i=1}^N \left(\frac{\alpha}{2} \left((\lambda_i^{(j)})^2 - (\lambda_i^{(k)})^2 \right) - i \left(\lambda_i^{(j)} - \lambda_i^{(k)} \right) \right). \quad (\text{S9})$$

Finally, the normalization factor, $1/\mathcal{N}_{J_\lambda^\alpha}$ is chosen such that $J_\lambda^\alpha = m_{\lambda^{(n)}} + \sum_{j=1}^{n-1} c_j m_{\lambda^{(j)}}$, i.e., the coefficient in front of $m_{\lambda^{(n)}}$ is one.

As an example, the explicit expression of J_{420}^2 is written as,

$$J_{420}^2 = \frac{1}{\mathcal{N}_{J_{420}^2}} \begin{vmatrix} m_{222} & m_{321} & m_{330} & m_{411} & m_{420} \\ -4 & 6 & 0 & 0 & 12 \\ 0 & -4 & 3 & 3 & 4 \\ 0 & 0 & -1 & 0 & 2 \\ 0 & 0 & 0 & -1 & 2 \end{vmatrix} \quad (\text{S10})$$

Compare the above equation to ϕ_6 that we previously obtained, we find that $\phi_6 = J_{420}^2$.

Similarly, we could conclude that $\phi_7 = J_{520}$, $\phi_8 = J_{530}$, $\phi_9 = J_{531}$.

MAPPING INITIAL STATE TO MONIMIAL BASIS

we start from an initial state

$$\Psi_{I,1} = \mathcal{N}_{I,1}^{-\frac{1}{2}} \prod_{i=1}^N \left(\sum_{m=1}^N c_m z_i^m \right) \prod_i e^{-|z_i|^2/2}, c_m = 1. \quad (\text{S11})$$

and project to different angular momentum channels

$$\Psi_{I,1} = \mathcal{N}_{I,1}^{-\frac{1}{2}} \left(\sum_l \psi_l \right) \prod_i e^{-|z_i|^2/2}. \quad (\text{S12})$$

We obtain that $\psi_l = \sum_\lambda \prod_i d_{\lambda_i} m_\lambda$.

For example for $N = 3$,

$$\psi_6 = d_2^3 m_{222} + d_3 d_2 d_1 m_{321} + d_3^2 d_0 m_{330} \quad (\text{S13})$$

$$\psi_7 = d_3^2 d_1 m_{331} + d_3 d_2^2 m_{322} \quad (\text{S14})$$

$$\psi_8 = d_3^2 d_2 m_{332} \quad (\text{S15})$$

$$\psi_9 = d_3^3 m_{333}. \quad (\text{S16})$$

Though the initial state could couple to angular momentum less than 6, we can safely ignore them since they have zero overlap with the final state. Finally, combining the equations

$$\langle \psi_6 | J_{\lambda(6)} \rangle = (-\eta)^3 O_c \langle J_{\lambda(6)} | J_{\lambda(6)} \rangle \quad (\text{S17})$$

$$\langle \psi_7 | J_{\lambda(7)} \rangle = (-\eta)^2 O_c \langle J_{\lambda(7)} | J_{\lambda(7)} \rangle \quad (\text{S18})$$

$$\langle \psi_8 | J_{\lambda(8)} \rangle = (-\eta) O_c \langle J_{\lambda(8)} | J_{\lambda(8)} \rangle \quad (\text{S19})$$

$$\langle \psi_9 | J_{\lambda(9)} \rangle = O_c \langle J_{\lambda(9)} | J_{\lambda(9)} \rangle \quad (\text{S20})$$

and with the condition $d_3 = 1$, we can solve for O_d , and d_i . We solve for O_d first from Eq. (S20), then solve for d_2 from Eq. (S19), etc. The solution is guaranteed because they are linear in each step. We obtain $O_d = -(9/220)$, $d_0 = -((41991\eta^3)/332750)$, $d_1 = ((3303\eta^2)/6050)$, $d_2 = -((81\eta)/55)$. Note, O_d differ the overlap $\langle \Psi_{I,1} | \Phi_{1,\eta} \rangle$ by a normalization factor $(\mathcal{N}_1 \mathcal{N}_{1,\eta})^{1/2}$.

TABLE S1. The coefficients d_i (c_i) are for the wave functions with one quasi hole excitation at η (one quasi hole excitation at origin and another at η). O_d (O_c) is the overlap of the initial wave function and the final state.

N	O_d	d_0	d_1	d_2	d_3	O_c	c_1	c_2	c_3	c_4
2	$-\frac{2}{7}$	$\frac{4\eta^2}{49}$	$-\frac{8\eta}{7}$			$3/10$	$-4\eta^2/25$	$-9\eta/10$		
3	$-\frac{9}{220}$	$-\frac{41991\eta^3}{332750}$	$\frac{3303\eta^2}{6050}$	$-\frac{81\eta}{55}$		$12/257$	$-138478\eta^3/16974593$	$2928\eta^2/66049$	$-264\eta/257$	
4	$\frac{8}{2377}$	$\frac{3571758875792\eta^4}{861946858349307}$	$-\frac{41724784088\eta^3}{120873209697}$	$\frac{20331502\eta^2}{16950387}$	$-\frac{13504\eta}{7131}$	$\frac{125}{28931}$	$-\frac{88255919558988767\eta^4}{1401147243843246242}$	$\frac{1768215130300\eta^3}{24215326878491}$	$\frac{132909825\eta^2}{837002761}$	$-\frac{35075\eta}{28931}$

GENERALIZATION TO TWO QUASI-HOLE STATE IN THE MAIN TEXT

The same analysis could be performed for the two quasihole state. We need to replace λ_i by $\lambda_i + 1$. Once we express $\Phi_{1,\eta}(\{z_i\})$, the state with one quasi-hole, in terms of Jack Polynomials, we could immediately rewrite the state with two quasi-holes, $\Phi_{2,\eta}(\{z_i\})$ also in terms of Jack Polynomials, since $\Phi_{2,\eta}(\{z_i\}) \sim (\prod_i z_i)\Phi_{1,\eta}(\{z_i\})$.

The normalization constants $N(\lambda)$ changes but everything else, including the total number of basis and the coefficients in front of the basis remains the same. Likewise, generalization to cones, e.g., replace λ_i by $3\lambda_i$ also only changes the normalization factors. Using Jack polynomial, we are able to calculate the coefficients for up to $N = 8$. The coefficients required to generate the one-quasi-hole and two-quasi-hole state for N up to 4 is summarized in table S1.

SOLUTIONS TO THE MASTER EQUATION

Here, we use dissipative dynamics on a cone as an example. Discussions can be straightforwardly generalized to a flat plane. We consider a cavity supporting states with angular momenta 3, 6, and 9. To simplify notations, the decay rate of the p -orbital has been taken as a constant in these angular momentum channels. As an example, we set $g/\Omega = 4.3/1.5$. We perform a time-dependent calculation using the master equation and find that an initial pure state of 2 photons decays into a density matrix that is a mixture of the vacuum, the one-body dark state $d_l^\dagger |vac\rangle$ with angular momentum $l = 3, 6$, and 9, and a two-body quasihole state $D^\dagger |vac\rangle = \frac{1}{\sqrt{6.2}}d_6^\dagger d_6^\dagger |vac\rangle - \sqrt{\frac{2.1}{3.1}}d_3^\dagger d_9^\dagger |vac\rangle$. Here $\lambda = \Omega/\sqrt{g^2 + \Omega^2} = 0.329$, and $d_l^\dagger = \lambda a_l^\dagger - \frac{g\lambda}{\Omega} r_l^\dagger$. To be more explicit, the density matrix of the final steady state reads $c_{vac} |vac\rangle \langle vac| + c_3 d_3^\dagger |vac\rangle \langle vac| d_3 + c_9 d_9^\dagger |vac\rangle \langle vac| d_9 + c_6 d_6^\dagger |vac\rangle \langle vac| d_6 + c_{tb} D^\dagger |vac\rangle \langle vac| D$. Because the initial two photons have angular momentum 6, $c_3 = c_9$. There are no off diagonal terms in the final density matrix.

For convenience, we define anti-dark state $\tilde{d}_l^\dagger = \frac{g\lambda}{\Omega} a_l^\dagger + \lambda r_l^\dagger$. We rewrite the initial photonic state $(a_6^\dagger)^2 |vac\rangle$ as a superposition of states that are proportional to $(\tilde{d}_6^\dagger)^2, \tilde{d}_6^\dagger d_6^\dagger, (d_6^\dagger)^2$. The first part decays completely. The second part decays to a one-body dark state of angular momentum 6 with probability of $2\lambda^2(1 - \lambda^2) = 0.19$, which is the majority of c_6 . The last part decays to the two-body quasihole state with the probability of $c_{tb} = \lambda^4/3.1 = 0.38\%$ and an anti quasihole state. The anti quasihole states decays into the one-body dark states with $l = 3, 6, 9$. The coefficients c_3, c_9, c_6 depend on the interaction strength and the decay rate. For example, for $\gamma = 2.3\Omega$ and $U_0 = 74\Omega$ [Fig. S2(a)], $c_3 = 0.0008$ and $c_6 = 0.2001$; for $\gamma = 2.3\Omega$ and $U_0 = 111\Omega$ [Fig. S2(b)], $c_3 = 0.0004$, and $c_6 = 0.201$; for $\gamma = 1.15\Omega$ and $U_0 = 111\Omega$ [Fig. S2(c)], $c_3 = 0.007$, and $c_6 = 0.190$.

The lines in Fig. S2 show the time-dependent coefficient, $c(t)$, of the density matrix. The blue lines denote $c_{tb}(t)$. Since it is the coefficient for the dark state, $c_{tb}(t)$ stays as a constant regardless of the interaction strength and the decay rate. The red, green, black lines denote c_3, c_6 , and c_{vac} , respectively. Changing the interaction strength [Fig. S2(a)] or the decay rate [Fig. S2(c)] leads to changes in c_3, c_6 , and c_{vac} .

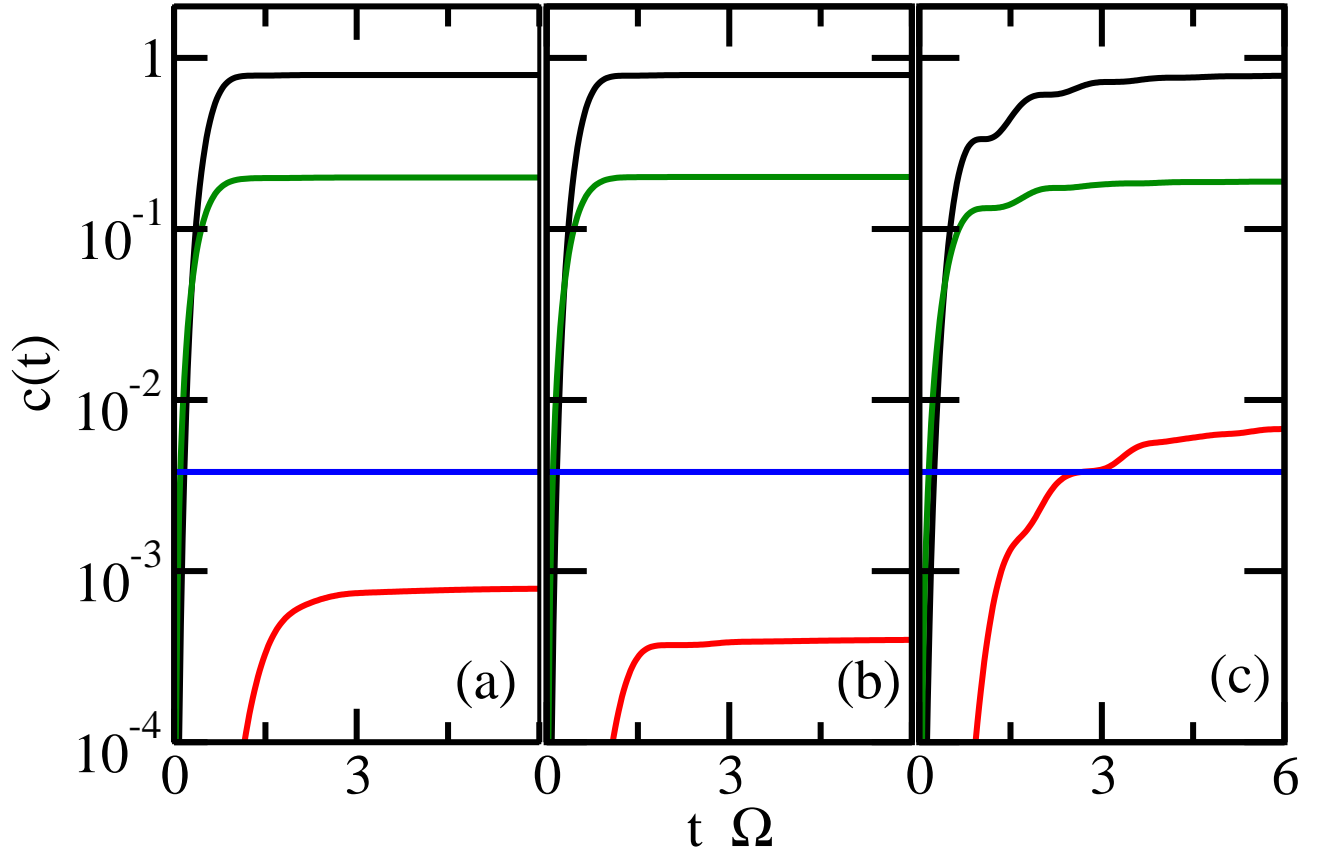


FIG. S2. The black, green, red, and blue lines shows the probability $c(t)$ for the diagonal density matrix elements $|vac\rangle\langle vac|$, $d_6^\dagger|vac\rangle\langle vac|d_6$, $d_3^\dagger|vac\rangle\langle vac|d_3$, $D^\dagger|vac\rangle\langle vac|D$ as a function of time. $d_9^\dagger|vac\rangle\langle vac|d_9$ is the same as $d_3^\dagger|vac\rangle\langle vac|d_3$. Panel (a) is for $\gamma = 2.3\Omega$ and $U_0 = 74\Omega$. Panel (b) is for $\gamma = 2.3\Omega$ and $U_0 = 111\Omega$. Panel (c) is for $\gamma = 1.15\Omega$ and $U_0 = 111\Omega$. Changing the interaction energy or decay rate do not change the two-body dark state at all but they affects the one-body states and vacuum state. From (a) to (b), changing U does not affect the decay to the one-body sector much, which is mainly governed by the decay rate in the p -orbitals.